Interleukin 10 controls the balance between tolerance, pathogen elimination and immunopathology in birds.

Dominique Meunier[1,5], Ricardo Corona-Torres[1,5], Kay Boulton[1], Zhiguang Wu[1], Maeve Ballantyne[1], Laura Glendinning[1], Anum Ali Ahmad[1], Dominika Borowska[1], Lorna Taylor[1], Lonneke Vervelde[1,3], Jorge del Pozo[1], Marili Vasilogianni[2], José Jaramillo-Ortiz[2], Gonzalo Sanchez-Arsuaga[2], Androniki Psifidi[2], Fiona Tomley[2], Kellie A. Watson[1], Michael J. McGrew[1], Mark P. Stevens[1], Damer P. Blake[2] and David A. Hume[1,4,✉]

1. The Roslin Institute & Royal (Dick) School of Veterinary Studies, University of Edinburgh, Easter Bush, Midlothian, EH25 9RG, United Kingdom.
2. The Royal Veterinary College Hawkshead Lane North Mymms Hatfield Hertfordshire AL9 7TA United Kingdom.
3. Current address: Royal GD Animal Health, Arnsbergstraat 7, 7418 EZ Deventer, The Netherlands.
4. Current address: Mater Research Institute-University of Queensland, Brisbane, Queensland 4102, Australia.
5. These authors contributed equally to the work.

✉ Corresponding author: david.hume@uq.edu.au

Keywords

IL10, Chicken, Inflammation, Primordial germ cells, Genome editing, *Campylobacter*, *Salmonella*, *Eimeria*

Abstract

Effective mucosal immunity in the intestine involves a fine balance between tolerance of the microbiome, recognition and elimination of pathogens, and inflammatory tissue injury. The anti-inflammatory cytokine IL10 regulates these processes in the intestines of mice and humans; the anti-inflammatory activity of IL10 is also conserved in birds. To determine the function of IL10 in avian mucosal immunity, we generated germ line modifications of the chicken *IL10* locus to abolish or reduce IL10 expression. *In vitro* analysis of macrophage response to lipopolysaccharide confirmed the loss of IL10 protein expression, the lack of dosage compensation in heterozygotes, and prevention of autocrine inhibition of nitric oxide production in homozygous IL10 knockout macrophages. IL10-deficiency significantly altered the composition of the caecal microbiome, but unlike IL10-deficient mice and humans, IL10-deficient chickens did not exhibit spontaneous colitis. Following experimental challenge with *Salmonella enterica* serovar Typhimurium or *Campylobacter jejuni* in IL10-deficient chickens, enhanced clearance of the pathogens was associated with elevated transcription of pro-inflammatory genes and increased infiltration of inflammatory cells into gut mucosa. In IL10-deficient chickens challenged with the parasite *Eimeria tenella,* pathogen clearance was accelerated but caecal lesions were more severe and weight gain was compromised. Neither the heterozygous IL10 knockout nor a homozygous IL10 enhancer mutation had a major effect on pathogen clearance or inflammation in any of the challenge models. Our findings highlight the intrinsic compromise in mucosal immune response and have important implications for the development of strategies to combat avian and zoonotic pathogens in poultry.

Introduction

Elimination of potential pathogens by the innate and acquired immune systems involves an intrinsic compromise between host protection and tissue injury that requires mechanisms to control the nature, magnitude, duration and specificity of effector pathways. A key component of specificity is the capacity to distinguish between pathogens and the commensal microbiome, and nowhere is this challenge more pressing than in the intestine. The anti-inflammatory cytokine, interleukin 10 (IL10), has long been recognized as an essential feedback regulator of intestinal inflammation in mammals (reviewed in (1)). IL10-deficient mice generated by homologous recombination developed spontaneous enterocolitis (2). Subsequent studies revealed that components of the intestinal microbiome were essential to development of pathology and determined the extent and location of lesions (3). In humans, homozygous mutations in genes encoding IL10 or its receptor, IL10RA, have been associated with early-onset inflammatory bowel disease (1).

In mammals, IL10 is produced by both myeloid and T and B lymphoid cells following activation by immune stimuli (1, 4), with subtle differences between mice and humans (5). In the specific context of the intestine, conditional deletion of the *IL10* and *IL10RA* genes in mice indicated that production of the ligand by macrophages was not required for pathology, consistent with T cells being the major source of intestinal IL10 (6, 7). By contrast, macrophage-specific deletion of the *IL10RA* gene encoding the IL10 receptor was sufficient to elicit spontaneous colitis in mice (8-10). The contribution of IL10 to feedback modulation of host defense is not restricted to the gut. There have been countless studies of the impact of IL10 deficiency in mouse parasite, bacterial, fungal and viral disease models (reviewed in (4)). The primary focus of these studies has been on the mitigation of immunopathology by IL10, with less attention given to pathogen elimination. By contrast to studies in mice, analysis of the quantitative importance of IL10 in other species has been largely correlative. Both ligand and receptor are conserved in vertebrates, and zebrafish has been discussed as a model for understanding

71 IL10 biology (11). Here we focus on the chicken, both a model vertebrate and an economically
72 important livestock species.

73 The original cloning and sequencing of chicken *IL10* cDNA and genomic DNA (12) described
74 the immunomodulatory activity of the recombinant protein on T cell production of interferon-
75 gamma (IFNγ), its regulated expression in T cells and macrophages *in vitro*, and increased
76 mRNA expression during parasite (*Eimeria maxima*) infection. Like the mammalian transcript,
77 chicken *IL10* mRNA contains multiple copies of the AUUUA instability motif in the 3'-
78 untranslated region (UTR). We and others have provided evidence that quantitative variation
79 in IL10 production may contribute to inter-individual or inter-breed variation in infectious
80 disease susceptibility in chickens (13-17). To test this hypothesis directly, and more generally
81 to determine the conservation of IL10 biological function across vertebrates, we have
82 generated germ line modifications of the chicken *IL10* locus that abolish or reduce IL10
83 expression. We describe the lack of dosage compensation in heterozygous mutation, and
84 present evidence that the reduced expression of IL10 leads to increased pathogen clearance
85 at the expense of increased inflammation.

86 **Results**

87 **Generation of IL10-deficient chickens**

88 The emergence of CRISPR/Cas9 technology and the ability to culture, cryopreserve,
89 genetically modify and subsequently transfer chicken primordial germ cells (PGCs) into sterile
90 surrogate host embryos has expedited the analysis of gene function in the chick (Figure 1A;
91 (18-21)). We used this approach to edit the *IL10* locus in chicken PGCs and create two
92 independent lines of IL10-deficient chickens (Figure 1). We first created an IL10 knockout
93 (IL10KO) line by introducing a premature in-frame stop codon in exon 1 of the *IL10* gene in
94 chicken PGCs, 75 bp downstream of the start codon (C26>*; Figure 1B and D, and SI
95 Appendix, Figure S1). To generate a potential expression hypomorph, we created an IL10-

96 Enhancer knockout (IL10EnKO) line by deleting a 533-bp genomic fragment encompassing a
97 non-coding sequence located approximately 2.3-2.8 kb upstream of the *IL10* transcription start
98 site, in chicken PGCs (Figure 1B-C and SI Appendix, Figure S2). This sequence was targeted
99 based upon alignment of sequences from multiple avian species that identified a core of 300
100 bp with conservation around 85%, containing perfectly conserved motifs for known
101 transcriptional regulators, including AP1, FOXP3 and members of the NFAT/ETS family (SI
102 Appendix, Figure S3). The size and species conservation of this element resembles the well-
103 characterized intronic enhancer of the *Csf1r* locus (22).

104 To create IL10KO and IL10EnKO chickens, male PGCs carrying the desired biallelic edit in
105 *IL10* exon 1 or in the putative *IL10* enhancer region (as validated by PCR and DNA
106 sequencing; Figure 1C-D and SI Appendix, Figure S4) were injected into iCaspase9 sterile
107 surrogate host embryos, in which a chemically inducible caspase 9 protein is expressed from
108 the PGC-specific *DAZL* locus, together with a GFP reporter (23). Embryos were treated with
109 the iCaspase9 activation chemical AP20187, incubated to hatch, and the resulting chicks were
110 raised to sexual maturity under specified pathogen-free (SPF) conditions at the National Avian
111 Research Facility (NARF). Mating of the iCaspase9 surrogate host cockerels to Rhode Island
112 Red (RIR) hens generated 100% IL10KO or IL10EnKO heterozygous (HET) offspring in the
113 first generation (G1; Figure 1A and SI Appendix, Table S1). Upon sexual maturity, G1 HET
114 birds were intercrossed to generate the second generation (G2) of IL10KO and IL10EnKO
115 wildtype (WT), HET and homozygous (HOM) birds for analyses. Both lines produced WT, HET
116 and HOM offspring at a 1:2:1 mendelian ratio (SI Appendix, Table S1).

117 **Confirmation of the IL10 mutation in bone marrow-derived macrophages**

118 Chicken bone marrow-derived macrophages (BMDMs) cultured in recombinant macrophage
119 colony-stimulating factor respond to bacterial lipopolysaccharide (LPS) by secreting IL10 that
120 can be detected by ELISA (24). The autocrine function of IL10 in this assay was demonstrated
121 by the addition of neutralizing anti-IL10 antibody, which amplified the expression of nitric oxide

122 synthase (NOS2) and production of nitric oxide (24). Figure 2A confirms the release of IL10
123 by LPS-stimulated BMDMs derived from WT embryos and the complete absence of detectable
124 IL10 release by BMDMs derived from IL10KO HOM embryos. The absence of IL10 was
125 associated with a significant increase in nitric oxide production that was not additive with the
126 impact of added anti-IL10 antibody (Figure 2B). Since IL10 mediates feedback control it is
127 conceivable that the loss of one functional allele could be compensated by increased
128 expression from the other allele. However, we found that expression of IL10 was reduced by
129 up to 50% in BMDMs derived from IL10KO HET embryos, with a corresponding partial impact
130 on nitric oxide production (Figure 2A-B). The impact of the IL10EnKO HOM mutation was
131 more variable between samples in both assays, but consistent with a partial expression
132 hypomorph (Figure 2A-B).

133 **Loss of IL10 does not lead to spontaneous immunopathology**

134 The IL10KO and IL10EnKO chicken lines were created and raised under SPF conditions in
135 the NARF SPF avian facility. Close monitoring of the WT, HET and HOM birds over several
136 months in that environment did not reveal any health issues or adverse phenotypes. The
137 IL10KO and IL10EnKO edits did not significantly affect the post-hatch growth of HET and HOM
138 birds compared to their respective WT controls (Figure 3A-B), although IL10EnKO HET and
139 HOM hens were overall heavier than IL10EnKO WT controls (Figure 3B). Regular gross post-
140 mortem examination of tissues and histopathological analyses of the gastrointestinal tract over
141 several months (using a semiquantitative scoring system (62)) revealed no evidence of
142 intestinal pathology in IL10KO HOM and IL10EnKO HOM birds compared to WT controls
143 (Figure 3C). These results are in contrast with the early onset colitis and failure to thrive
144 phenotypes observed in IL10-deficient mouse models in both conventional and SPF
145 environments (2, 9, 25, 26).

146 Spontaneous colitis in *Il10*$^{-/-}$ mice is associated with and dependent upon dysbiosis in the
147 intestinal microbiome (27-29). We compared the caecal microbiome of IL10KO WT and HOM

148 birds at 4 weeks of age using 16S rDNA V3-V4 hypervariable amplicon sequencing as
149 described (30, 31). The caecal microbiome of both genotypes was dominated by the phylum
150 *Firmicutes* (SI Appendix, Figure S5A) and the most abundant genera were *Lactobacillus* and
151 *Faecalibacterium* (SI Appendix, Figure S5B). Linear discriminant analysis (LDA) Effect Size
152 (LEfSe) analysis showed enrichment of the phylum *Firmicutes* and the genera
153 *Defluviitaleaceae_UCG-011* and *Paludicola* in the IL10KO HOM group, while the phylum
154 *Bacteroidota* and the genera *Alistipes* and *UCG_008* were enriched in the WT group (SI
155 Appendix, Figure S5C). Principal component analyses showed clear separation of the
156 microbial communities based on beta diversity (SI Appendix, Figure S5D, $R^2 = 0.25$, $P =$
157 0.017). These findings confirm that mucosal IL10 regulates the composition of the chicken
158 microbiome.

159 To evaluate a potential environmental impact on the phenotype of IL10-deficient birds, a
160 cohort of IL10KO WT and HOM birds was hatched and raised in the NARF conventional avian
161 facility. IL10KO HOM birds remained healthy in that environment as they aged. Post-growth
162 hatch rates were comparable between IL10KO WT and HOM hens, with the exception of a
163 marginal effect on growth that resolved with age (Figure 3D). Whilst there was no statistically
164 significant evidence of overt intestinal pathology in IL10KO HOM birds compared to WT
165 controls (Figure 3E), cellular infiltration scores were overall significantly higher in IL10KO WT
166 and HOM birds raised in a conventional facility as opposed to a SPF environment (Figure 3F).

167 Two important differences exist between the IL10KO mouse and chicken models. Firstly, the
168 birds are outbred. Most mouse studies are conducted on an inbred background and the impact
169 of the *IL10* mutation is strain-specific (26). Secondly, chickens in the NARF conventional avian
170 facility are routinely immunised against major avian pathogens (SI Appendix, Table S2). The
171 original analysis of IL10-deficient mice revealed little impact on T cell-dependent antibody
172 responses (2). We measured antibody titres in 29-weeks old IL10KO WT and HOM birds
173 raised in the NARF conventional facility for 7 of the pathogens that the birds were vaccinated

174 against (SI Appendix, Figure S6): avian encephalomyelitis virus (AEV), chicken anaemia virus
175 (CAV), duck adenovirus (the agent of egg drop syndrome, EDS), infectious bursal disease
176 virus (IBDV), infectious bronchitis virus (IBV), infectious laryngotracheitis virus (ILTV), and
177 Newcastle disease virus (NDV). The administration schedule, nature and delivery mode of
178 these vaccines is summarised in SI Appendix, Table S2**.**

179 Statistical analyses revealed differences in vaccine response between IL10KO WT and HOM
180 birds. Antibody titres to AEV and IBDV were significantly lower in IL10KO HOM birds
181 compared to WT controls, whereas those to EDS and IBV were significantly higher in IL10KO
182 HOM birds compared to WT controls (SI Appendix, Figure S6). AEV and IBDV vaccination
183 were carried out with live vaccines delivered in the drinking water, whereas EDS and the last
184 dose of IBV vaccination were done with inactivated vaccines given by intramuscular injection
185 (SI Appendix, Table S2). Antibody titres to CAV, ILTV and NDV were not significantly different
186 between IL10KO HOM birds and WT controls (SI Appendix, Figure S6).

187 **The impact of IL10 deficiency on the response to enteric bacterial infection**

188 *Campylobacter jejuni* (*C. jejuni*) and non-typhoidal *Salmonella* are zoonotic diarrhoeal
189 pathogens of global importance (32). Breed-specific pathology associated with *C. jejuni*
190 infection in chickens was associated with relatively low caecal *IL10* mRNA (33). Similarly,
191 IL10-deficient C57BL/6J mice exhibited severe inflammation in the caecum and colon upon
192 *C. jejuni* infection, whereas congenic wild-type mice were persistently colonised in the
193 absence of gut pathology (34). A similar outcome was reported in IL10-deficient mice infected
194 with *Salmonella* Typhimurium (*S*. Typhimurium) (35).

195 To study the role of IL10 during *Campylobacter* infection in chickens, two cohorts of 20 IL10KO
196 WT, HET or HOM chickens obtained from the NARF SPF avian facility were inoculated at 14
197 days-old with 10^2 colony forming units (CFU) *C. jejuni* strain M1 and analysed 1- and 2-weeks
198 post-infection. The dose of strain M1 used is the lowest needed to achieve reliable caecal

199 colonisation (36). In the first cohort, colonisation of the caeca by *C. jejuni* in IL10KO HOM
200 birds was significantly lower at 1-week post-infection, with a median of 4.8 $\log_{10}$ CFU g^{-1}
201 compared to >9 $\log_{10}$ CFU g^{-1} in WT birds Figure 4A). However, this was not sustained and
202 by 2-weeks post-infection all groups had caecal colonisation at >9 $\log_{10}$ CFU g^{-1} (Figure 4A).
203 In the second cohort, median counts were not statistically different between IL10KO HOM and
204 WT birds at 1-week post-infection, but caecal colonisation decreased by ~2 $\log_{10}$ CFU g^{-1} in
205 IL10KO HOM birds at 2-weeks post-infection relative to WT birds (Figure 4A). The IL10KO
206 HET birds did not differ significantly from WT in either cohort (Figure 4A). Histopathological
207 analysis revealed that the caecal mucosa of IL10KO HOM birds presents with significantly
208 increased numbers of lymphocytes and plasma cells, admixed with infiltrating heterophils,
209 when compared to WT and IL10KO HET birds in both cohorts (SI Appendix, Figures S7 and
210 S8). To confirm the apparent hyperinflammatory response in IL10KO HOM birds, we used
211 multiplex quantitative reverse transcriptase-PCR (qRT-PCR) to measure expression of
212 immunity-related genes in the caecum, as described (37). In both cohorts we detected large
213 increases in expression of pro-inflammatory cytokines, chemokines and other effectors,
214 notably *Nos2*, in the IL10KO HOM caecum relative to WT (Figure 4B).

215 To test the role of IL10 in response to *Salmonella* infection, groups of 20 IL10KO WT, HET or
216 HOM chickens were inoculated at 14 days-old with 10^8 CFU *S*. Typhimurium strain ST4/74
217 nal^R (38). The impact of lack of IL10 on bacterial burden in caecum, liver and spleen was
218 marginal at 1 week, but by 2 weeks the majority of IL10KO HOM birds had eliminated the
219 pathogen, whereas WT birds retained bacteria in both caecum and spleen (Figure 4C).
220 Enhanced lymphoplasmacytic and heterophil infiltration was observed in the ileum and
221 caecum of IL10KO HOM compared to WT or IL10KO HET birds at both intervals after *S*.
222 Typhimurium infection (SI Appendix, Figure S9). As observed following the *C. jejuni* challenge,
223 analysis of inflammatory gene expression by multiplex qRT-PCR revealed a substantial
224 increase in response in the IL10KO HOM birds relative to WT (Figure 4D). Volcano plots

225 showing the direction and magnitude of gene expression differences detected between
226 IL10KO HOM and WT birds following bacterial infection are shown in SI Appendix, Figures
227 S10 and S11. In summary, the absence of IL10 leads to a sustained increase in inflammation
228 in response to enteric bacterial infection that is also associated with more effective clearance.

229 **The impact of IL10 deficiency on the outcome of enteric protozoan infection**

230 *Eimeria tenella* (*E. tenella*) is one of ten protozoan parasite species that can cause coccidiosis
231 in chickens (39). *Eimeria* infection of chickens induces a robust IFNγ-driven immune response
232 with evidence of higher IL10 expression associated with increased susceptibility (12, 40).
233 Following an initial titration, an infectious dose of 7000 sporulated *E. tenella* oocysts per bird
234 was set as the standard challenge, as this induced measurable phenotypes in pathology,
235 performance, and parasite replication in the absence of overt disease in WT birds. Oral
236 challenge with this or a mock dose was administered to cohorts of 10 IL10KO HOM and
237 IL10EnKO HOM chickens and corresponding WT and HET controls on day 21 post-hatch. The
238 outcomes are shown in Figure 5**.** Average parasite replication was determined by quantitative
239 PCR (qPCR) as the ratio of parasite genomes detected per host genome in total caecal tissue
240 collected six days post-infection. Parasite burden was almost ablated in IL10KO HOM and
241 significantly reduced in IL10EnKO HOM chickens compared to their respective WT controls,
242 whereas HET mutations had no significant effect in either case (Figure 5A-B). Histology
243 confirmed reduced parasite replication in IL10KO HOM chickens, with dense populations of
244 late-stage gametocytes observable in WT caecal tissues and correspondingly very sparse
245 numbers in IL10KO HOM chickens (Figure 5C-D). This selective reduction of parasite burden
246 in IL10KO HOM chickens was associated with a significant increase in caecal lesion score
247 and a substantial reduction in body weight gain over the 6-day challenge interval (Figure 5E
248 and G). By contrast, both IL10KO HET and IL10EnKO HOM and HET (each anticipated to
249 reduce IL10 expression) showed reduced caecal lesion scores and had no effect on body
250 weight gain compared to their respective WT controls (Figure 5E-H).

251 To better characterise the differences in pathology, performance and parasite replication
252 detected between IL10KO WT and HOM chickens, we undertook a time course study,
253 analysing parasite burden by qPCR at 0-, 2-, 4-, 6-, 8- and 10-days post-infection. In parallel,
254 excreted oocysts per gram (OPG) were counted in litter samples collected from IL10KO HOM
255 and WT groups during the period of peak oocyst excretion at 7-, 8- and 9-days post-infection.
256 Figure 6A confirms the greatly reduced *E. tenella* replication in IL10KO HOM, that was
257 reflected in corresponding reduced excretion of oocysts (Figure 6B). Lesions associated with
258 *E. tenella* infection were accelerated in IL10KO HOM chickens compared to WT (Figure 6C).
259 The adverse impact of IL10KO HOM on body weight gain was sustained to day 8 and showed
260 signs of recovery by day 10 (Figure 6D), likely due to complete pathogen elimination (Figure
261 6A). Consistent with the mild inflammatory cell infiltration in IL10KO HOM birds noted in Figure
262 5D, inflammatory gene expression was elevated in the caecum prior to challenge (Day 0). The
263 greatest difference in IL10KO HOM birds relative to WT was detected on day 6, during the
264 period of peak pathology (Figure 6C and E). Volcano plots showing the direction and
265 magnitude of gene expression differences detected between IL10KO HOM and WT birds
266 following *E. tenella* infection are shown in SI Appendix, Figure S12, highlighting genes
267 associated with inflammation (*Il6*) and lysosomes (*Hps5*). Transcription of genes associated
268 with movement of molecules across membranes (*Pkd2l1, Abcg2*) and tubulin production
269 (*Tubat*) was lower in IL10KO HOM birds 6 days post-infection.

270 **Discussion**

271 An intrinsic compromise exists between effective host defence leading to pathogen elimination
272 and the induction of immune-mediated pathology. The central importance of IL10 in mediating
273 this balance has been studied extensively in the mouse, notably in the context of parasite
274 infections (1, 4, 5, 11, 41). The regulatory function of IL10 is especially important in preventing
275 inappropriate responses to the intestinal microbiome with the potential to drive spontaneous
276 enterocolitis (2, 8, 10, 26). Here we have generated two *IL10* mutations in the chicken genome,

277 a definitive knockout and a putative enhancer mutation. Notwithstanding the development of
278 robust technologies based upon CRISPR/Cas9, the development of models of immune
279 deficiency in chickens remains time consuming and logistically challenging, and relatively few
280 informative mutations have been generated (20, 42). The enhancer mutation was intended to
281 generate a quantitative impact on IL10 expression to model selection for reduced expression
282 in production lines of birds. Based upon the mouse *Il10*$^{-/-}$ phenotype, we also anticipated a
283 possible severe post-hatch failure to thrive due to spontaneous colitis in IL10KO HOM chicks.
284 An unexpected outcome was the discovery that the IL10KO in chicken is not dosage
285 compensated, therefore the HET provides a second model of the impact of reduced
286 expression. In overview, neither the IL10KO HET nor the IL10EnKO HOM had a large effect
287 on pathogen clearance or inflammation in either of the challenge models, indicating that IL10
288 biology is not highly sensitive to changes in expression of the magnitude that has been
289 detected in individual lines of commercial broilers and layers (14, 43, 44).

290 Detailed analysis of the IL10KO HOM birds in SPF or conventional avian facilities revealed no
291 evidence of spontaneous intestinal inflammation or compromised body weight gain, and only
292 a small and inconsistent effect on specific antibody responses to routine live or inactivated
293 vaccines. Since spontaneous colitis in mice depends upon resident enteric bacteria (3), it is
294 possible that the difference compared to the rodent models lies in the nature of the chicken
295 intestinal microbiome (45). In any case, the results indicate that deletion of IL10 from the
296 genome or selection in favour of low IL10 expression alleles (14, 17, 43, 44) need not
297 necessarily affect production traits.

298 In both the bacterial challenge models, and in the *Eimeria* challenge, the response of IL10KO
299 HOM bird highlights for the first time in a non-rodent species the compromise between
300 pathogen elimination and pathology. Accelerated pathogen clearance is associated with
301 increased inflammatory gene expression and local inflammation, and in the case of *Eimeria*,
302 reduced body weight gain. The models we have chosen are not lethal and there is effective

303 pathogen clearance even in WT birds. Findings with *Campylobacter* in IL10KO HOM birds are
304 consistent with elevated intestinal inflammation in a broiler breed with relatively low IL10
305 expression, albeit a significant reduction in caecal colonisation relative to breeds with higher
306 IL10 expression was not observed (33). In mammals, *Salmonella* has been reported to gain a
307 competitive advantage from intestinal inflammation, both owing to availability of tetrathionate
308 that *Salmonella* can uniquely use as a respiratory electron acceptor (46) and remodelling of
309 the indigenous microbiota (47). It is unclear if *Salmonella* derives the same benefits during
310 colonisation of the avian intestine and the counts of viable bacteria recovered from the caeca
311 of WT and IL10KO HOM birds can only be interpreted as the balance of bacterial growth and
312 killing.

313 Our results with *Eimeria* are relevant to commercial studies aimed at targeting IL10 to mitigate
314 disease. Coccidiosis has been estimated to exert costs in excess of £10 billion every year to
315 the chicken production industry (48), with *E. tenella* among the most common and pathogenic
316 species (49, 50). Feeding neutralizing anti-IL10 antibody to chickens during *Eimeria* infection
317 was reported to mitigate reduced body weight gain (BWG) but had an inconsistent impact on
318 parasite replication and pathology (51, 52). Similarly, feeding antibody to IL10 receptor 2 (but
319 not receptor 1) reduced lost BWG, but had no effect on oocyst shedding (53). Feeding
320 chickens genetically modified corn (*Zea mays*) expressing IL10 improved BWG and reduced
321 oocyst shedding and caecal lesions (54). These results are consistent with the phenotypes
322 associated with a reduction, rather than complete absence, of IL10 observed here.

323 Given the excessive inflammatory activation we observed in non-lethal infections, and the
324 literature in mice, IL10KO HOM birds or hypomorphs might be hyper-sensitive to more virulent
325 bacterial infections and viral pathogens, such as avian influenza, that can elicit a cytokine
326 storm. On the other hand, they may be primed for a more rapid and effective response. These
327 possibilities can now be tested using the models we have developed.

328 **Materials and Methods**

329 **Animals**

330 All chicken lines used in this study were bred and maintained at the National Avian Research
331 Facility (NARF), University of Edinburgh, under UK Home Office Establishment Licence and
332 in compliance with the Animals (Scientific) Procedures Act (ASPA) 1986. All regulated
333 procedures were approved by local ethical review committees and carried out by UK Home
334 Office Personal Licence holders under UK Home Office Project Licences 70/8528 and
335 PP9565661 (creation and maintenance of genetically altered chicken lines), PCD70CB48
336 (*Campylobacter* and *Salmonella* challenges performed at the Moredun Research Institute)
337 and PDAAD5C9D (*Eimeria* challenges performed at the Royal Veterinary College). Animals
338 were humanely culled in accordance with Schedule 1, ASPA 1986.

339 The Rhode Island Red (RIR) line was maintained as a closed outbred population in the NARF
340 specified pathogen-free (SPF) avian facility. The CSF1R-eGFP line (55) was created and
341 maintained on a Hy-Line background in the NARF conventional avian facility by HOM x HOM
342 crosses; CSF1R-eGFP fertile eggs were used for PGC derivation. The iCaspase9 line (23)
343 was created and maintained on a RIR background in the NARF SPF avian facility by crossing
344 iCaspase9 HET cockerels to RIR hens; iCaspase9 fertile eggs were used as hosts for PGC
345 injection. The IL10KO and IL10EnKO lines were created in the NARF SPF avian facility and
346 maintained on a mixed Hy-Line / RIR background by crossing iCaspase9 surrogate host
347 cockerels carrying gene-edited PGCs (generation G0) to RIR hens to produce the first
348 generation of IL10KO HET and IL10EnKO HET chickens (G1); the second generation (G2) of
349 IL10KO and IL10EnKO chickens was obtained by crossing G1 HET cockerels to G1 HET hens
350 from each line, resulting in WT, HET and HOM offspring.

351 **Chicken PGC derivation and culture**

352 PGC lines were derived from blood collected from CSF1R-eGFP HOM embryos at
353 Hamburger-Hamilton (HH) stage 16 and expanded in FAOT medium as previously described
354 (56). A W-chromosome-specific PCR (57) was used to determine the sex of the PGC lines.
355 PGC lines were tested for *Mycoplasma* contamination by PCR using primers specific for
356 *Mycoplasma synoviae* (MS; Myco5_14713A and Myco3_14709) and *Mycoplasma*
357 *gallisepticum* (MG; Myco5_14712 and Myco3_14709); see SI Appendix, Table S3 for primer
358 sequences.

359 **CRISPR plasmid, guide RNAs and ssODN donor**

360 Guide RNAs (gRNAs) were designed using CHOPCHOP (58) and CRISPOR (59) and cloned
361 into the High Fidelity CRISPR/Cas9 plasmid HF-PX459 V2.0 (60) as described previously
362 (61). A gRNA (ggIL10_exon1_g3) and a 143-bp single-stranded oligonucleotide DNA (ssODN;
363 IL10_exon1_HDRoligo2; IDT Ultramer™ DNA Oligonucleotide) containing a STOP codon
364 (TAG) and AvrII restriction site (CCTAGG), were used to edit *IL10* exon 1. Two gRNAs
365 (IL10_enhancer_guide1 and IL10_enhancer_guide2) were used in combination to delete the
366 *IL10* putative enhancer region. See SI Appendix, Table S4 for gRNA and ssODN sequences.

367 **PGC transfection and screening**

368 To edit *IL10* exon 1, 200,000 CSF1R-eGFP male PGCs were transiently transfected with 1.5
369 µg gRNA plasmid ggIL10_exon1_g3 and 10 pmol ssODN IL10_exon1_HDRoligo2. To delete
370 the *IL10* putative enhancer region, 200,000 CSF1R-eGFP male PGCs were transiently
371 transfected with 1.0 µg gRNA plasmid IL10_enhancer_guide1 and 1.0 µg gRNA plasmid
372 IL10_enhancer_guide2. Transient transfections were performed with Lipofectamine 2000
373 (Invitrogen), followed by treatment with 0.4 µg/mL puromycin to enrich for transfected PGCs,
374 as previously described (60). Bulk PGC populations were screened by PCR to confirm the
375 presence of the desired IL10KO or IL10EnKO edits. Single-cell clonal populations were

376 subsequently expanded as previously described (60) and screened by PCR and sequencing.
377 Primers IL10_Exon1_F4 and IL10_Exon1_R4 were used to amplify a 1826-bp fragment
378 encompassing *IL10* exon 1, followed by digestion with AvrII to identify PGCs carrying the
379 IL10KO edited allele (SI Appendix, Figure S4A); primers IL10_Exon1_F1 and IL10_Exon1_R1
380 were subsequently used to sequence the *IL10* exon 1 fragment. Primers IL10-Enhancer_F2
381 and IL10_Enhancer_R2 were used to amplify and sequence a fragment encompassing the
382 *IL10* putative enhancer region (SI Appendix, Figure S4C). See SI Appendix, Table S3 for
383 primer sequences and expected fragment sizes. PGCs were transfected and cultured under
384 SPF conditions and regularly tested for mycoplasma contamination, as described above.

385 **Generation of surrogate host chickens and establishment of the IL10KO and IL10EnKO**
386 **lines under SPF conditions**

387 Male PGCs carrying the desired IL10KO or IL10EnKO biallelic edits were injected into
388 iCaspase9 embryos at HH stage 16, together with the iCaspase 9 activator AP20187 (Takara
389 Bio) as previously described (23), to create surrogate host cockerels carrying IL10KO HOM
390 or IL10EnKO HOM germ cells (G0 founders); all manipulations were performed under SPF
391 conditions in the NARF SPF avian facility. G0 founders were hatched and raised to sexual
392 maturity in negative pressure isolators and released to floor pens at 22 weeks. The SPF status
393 of the G0 founders was externally assessed at three timepoints (10-, 20- and 30-weeks post-
394 hatch) by screening for 17 different pathogens (Sci-Tech Ireland; SI Appendix, Table S5).

395 G0 founder cockerels were bred to RIR hens to produce the first generation of IL10KO HET
396 and IL10EnKO HET chickens (G1); the second generation (G2) of IL10KO and IL10EnKO
397 chickens was obtained by crossing G1 HET cockerels to G1 HET hens, resulting in IL10KO
398 and IL10EnKO WT, HET and HOM offspring. All G1 and G2 chicks were genotyped by PCR
399 using genomic DNA extracted from chorioallantoic membrane or 4-μL blood samples as
400 previously described (23). Primers IL10_Exon1_F1 and IL10_Exon1_R1 were used to amplify
401 a 246-bp fragment encompassing *IL10* exon 1, followed by digestion with AvrII to identify the

402 IL10KO WT and edited alleles (SI Appendix, Figure S4B). Primers IL10-Enhancer_F2 and
403 IL10_Enhancer_R2 were used to amplify the IL10EnKO WT and edited alleles (SI Appendix,
404 Figure S4D). Primers LTR_U3_F, 235_F and 235_R were used to amplify the CSF1R-eGFP
405 WT and transgenic alleles. See SI Appendix, Table S3 for primer sequences and expected
406 fragment sizes. The SPF status of G1 and G2 chickens was verified at point of lay (20-24
407 weeks) and at end of life (around 40 weeks).

408 **Animal monitoring, post-mortem examination and histopathological analyses under**
409 **SPF and conventional conditions**

410 All IL10KO and IL10EnKO chicks hatched in the NARF SPF avian facility were closely
411 monitored for signs of reduced growth, health issues, adverse phenotypes or unexpected
412 behaviours. All chicks were weighed daily in the first week post-hatch and twice a week until
413 four weeks; a small cohort of G2 IL10KO and IL10EnKO chicks was subsequently weighed
414 weekly, up to a maximum of 30 weeks. Post-mortem examination of one WT and one HOM
415 bird from both IL10KO and IL10EnKO lines was performed monthly from 16 to 40 weeks, with
416 a particular focus on the gastrointestinal tract. Tissue samples from the proximal colon, ileum
417 and duodenum were collected for histopathological analyses at all timepoints and scored in a
418 blinded manner using a semiquantitative scoring system (62) to grade the extent of destruction
419 of normal mucosal architecture (0-3), the presence and degree of cellular infiltration (0-3), the
420 extent of muscle thickening (0-3), the presence or absence of crypt abscesses (0-1), and the
421 presence or absence of goblet cell depletion (0-1), for a maximum possible score of 11.

422 In addition to animals raised in the NARF SPF avian facility, a single cohort of IL10KO chicks
423 was hatched in the NARF conventional avian facility and closely monitored as described
424 above. Post-mortem examination of one WT and one HOM IL10KO birds was performed
425 monthly from 10 to 50 weeks, with a particular focus on the gastrointestinal tract. Tissue
426 samples from the proximal colon, duodenum and caecum were collected for histopathological
427 analyses and scored as described above.

428 **Generation of bone marrow-derived macrophage from chicken embryos**

429 Bone marrow cells were isolated from the tibias and femurs of Day 18 embryos (by pooling
430 three embryos of the same genotype per sample) by flushing the bone marrow through a 40
431 µm cell strainer with RPMI-1640 medium (Sigma R5886) supplemented with 10% fetal bovine
432 serum ultra-low IgG (Gibco 011-90035M), 2 mM L-glutamine (Gibco 25030081) and 0.1X
433 penicillin/streptomycin (Gibco 15140122) using a syringe and blunt needle. Bone marrow cells
434 were washed, resuspended at $1x10^6$ cells/mL in supplemented RPMI-1640 medium, seeded
435 at 1 mL per well in 6-well plates or 150 µL per well in 96-well plates, and cultured for 7 days
436 at 41°C, 5% CO_2 in the presence of 200 ng/mL colony stimulating factor-1 (CSF-1) to induce
437 formation of bone marrow-derived macrophages (BMDM). Cell culture supernatants were
438 subsequently used for capture ELISA and nitric oxide assay, as detailed below.

439 **Detection of IL10 by capture ELISA**

440 On day 7 of culture, BMDMs cultured in 6-well plates were stimulated with 0.5 µg/mL
441 lipopolysaccharide (LPS from *E. coli* O55:B5; Sigma L2880) for 2 hours at 41°C, 5% CO_2 to
442 induce IL10 expression; supernatants were then harvested and IL10 protein levels were
443 measured by capture ELISA, as described previously (24). Briefly, assay plates were coated
444 with 3 µg/mL capture antibody (ROS-AV164; (24)) incubated overnight at 4°C, washed and
445 blocked. Plates were then incubated with recombinant IL10 standards or 50 µl of 10-fold
446 diluted cell culture supernatants, followed by incubation with 1 µg/mL biotinylated detection
447 antibody (ROS-AV163; (24)) and then incubation with Pierce™ High Sensitivity Streptavidin-
448 HRP (1:5000; Thermo Fisher Scientific, cat #34028), before adding 1-Step™ TMB ELISA
449 Substrate Solution (Thermo Fisher Scientific, cat #21130) and then sulfuric acid stop solution.
450 Absorbance was measured at 450 nm (550 nm as a reference) in a SpectraMax 250
451 microplate spectrophotometer system (Molecular Devices, Sunnyvale, CA, USA). Data were
452 fitted with GraphPad Prism 7.0 using a second-order polynomial (quadratic) model; statistical
453 significance was calculated using two-tailed unpaired t tests.

454 **Nitric oxide assay**

455 On day 7 of culture, BMDMs cultured in 96-well plates were stimulated with 0.5 µg/mL LPS in
456 the presence or absence of 2.5 µg/mL neutralizing anti-IL10 antibody (ROS-AV163; (24)) for
457 24 hours at 41°C, 5% CO_2; supernatants were then harvested and nitrite levels were
458 measured by Griess assay, according to the manufacturer's instructions (Promega G2930);
459 absorbance was measured at 550 nm. Statistical significance was calculated using two-tailed
460 unpaired t tests.

461 **Response to vaccination**

462 IL10KO WT and HOM chicks hatched and raised in the NARF conventional avian facility were
463 vaccinated following the routine vaccination schedule in place in the facility (SI Appendix,
464 Table S2). One-mL blood samples were collected from the brachial vein of 29-weeks old hens
465 and sent fresh to Sci-Tech Ireland for antibody titre measurements by ELISA. Statistical
466 significance was calculated using Mann-Whitney U tests.

467 **Microbiome analysis**

468 Caecal contents were harvested from 4-weeks old IL10KO WT and HOM chicks raised in the
469 NARF SPF avian facility. DNA isolation, amplification of the V3-V4 region of the 16S rDNA
470 gene and pair-end sequencing were performed as described previously (31). Raw reads were
471 quality assessed using fastQC, and the DADA2 plugin in QIIME2 was used to generate an
472 ASVs table against the SILVA138 database. Alpha diversity and weighted uniFrac distances
473 were calculated using the Phyloseq package, while Bray-Curtis metrics were generated using
474 the vegan package. PERMANOVA (Bray-Curtis) analysis was conducted to test for significant
475 effects of the group on overall microbiome community composition. LEfSe analysis was
476 performed to identify differentially abundant phyla and genera between both groups using a
477 linear discriminant analysis (LDA) score equal to 4 as a threshold value. *P* values were

478 declared significant at $P < 0.05$. The sequencing data have been deposited in the European
479 Nucleotide Archive (ENA) at EMBL-EBI under accession number PRJEB71960.

480 **Bacterial strains**

481 *Campylobacter jejuni* strain M1 was used as the minimum number of viable bacteria required
482 for reliable intestinal colonisation of chickens has been defined (36). Strain M1 was grown on
483 charcoal cefoperazone deoxycholate agar (CCDA) at 41 °C for 48 hours in a microaerophilic
484 atmosphere (90 % N_2, 5 % CO_2 and 5 % O_2). For challenge, 10 mL of Mueller Hinton broth
485 was inoculated with single colonies and incubated for 16 hours with shaking at 41 °C in the
486 same atmosphere. Prior to inoculation, bacteria were confirmed to have spiral morphology
487 and to be motile by phase contrast microscopy. Cultures were diluted in phosphate-buffered
488 saline (PBS) based on a standard curve of colony-forming units (CFU/mL) relative to optical
489 density at 600 nm and inocula were retrospectively confirmed by plating serial ten-fold
490 dilutions onto CCDA. A spontaneous nalidixic acid-resistant mutant of *Salmonella enterica*
491 serovar Typhimurium strain 4/74 was used, as its colonisation kinetics are well defined in
492 chickens (38). This was cultured on Luria Bertani (LB) agar containing 20 µg/mL nalidixic acid
493 at 37 °C overnight and a single colony was transferred to LB broth with nalidixic acid and
494 incubated at 37 °C with shaking for 20 hours. 100 µL of this culture was used for inoculation
495 and the number of viable bacteria given was determined retrospectively by plating serial ten-
496 fold dilutions onto LB agar.

497 **Experimental infection of chickens**

498 Animal experiments using *Campylobacter* or *Salmonella* were conducted at the Moredun
499 Research Institute. Birds were provided with access to water and irradiated feed based on
500 vegetable protein *ad libitum*. Groups of 20 to 22 birds of each genotype (IL10KO WT, HET,
501 HOM) were wing-tagged for identification and separately housed in biosafety level 2 facilities
502 from day 7 of age in colony cages. At 14 days of age, birds were inoculated by oral gavage

503 with 100 µL of bacterial suspension. In two separate trials with *C. jejuni*, birds were inoculated
504 with $1x10^2$ CFU of strain M1. In a single trial with *S.* Typhimurium, birds were inoculated with
505 $1x10^8$ CFU of strain 4/74 nal^R. At 7 days post-inoculation, half of the birds in each group were
506 euthanised by cervical dislocation. The remainder of the birds were euthanised at 14 days
507 post-inoculation. On post-mortem examination, samples from the ileum and the distal end of
508 the caecum were stored in RNA*later*® or fixed in 10% neutral-buffered formalin for
509 histopathology. The contents of the caeca were pooled at the bird level, homogenised in PBS,
510 and ten-fold serial dilutions cultured on CCDA at 41 °C in a microaerophilic atmosphere to
511 enumerate CFU/g of *C. jejuni* or MacConkey agar containing 20 µg/mL nalidixic acid at 37 °C
512 aerobically to enumerate CFU/g of *Salmonella*.

513 **Histopathology**

514 Formalin-fixed tissue samples were embedded in paraffin, sectioned, mounted on glass slides,
515 and stained by haematoxylin-eosin (HE) staining. Histopathological analyses were performed
516 by a certified veterinary pathologist blind to the genotype of individuals and the inoculum.
517 Samples of ileum and caecum were assessed for the presence of lymphoplasmacytic and
518 heterophil infiltration on a scale of 0 to 5 (where infiltration is 0 normal, 1 slight, 2 mild, 3
519 moderate, 4 marked or 5 severe).

520 **RNA extraction and multiplex PCR**

521 Caecal tissue samples in RNA*later*® were homogenised with a hand-held tissue homogeniser
522 and RNA was extracted using RNeasy kit following the instructions from the manufacturer
523 (QIAGEN). The concentration and integrity of the RNA were respectively analysed using a
524 NanoDrop microvolume spectrophotometer and TapeStation automated electrophoresis
525 system. Reverse transcription, preamplification and high-throughput quantitative PCR (qPCR)
526 for avian immune-related transcripts and reference genes were performed as previously

527 described using a 96.96 Dynamic Array IFC for Gene Expression ((37); Standard BioTools,
528 San Francisco, CA, United States).

529 **Parasites**

530 Animal experiments using *Eimeria* were conducted at the Royal Veterinary College, using
531 chicks hatched at the NARF SPF avian facility. All chickens were provided with access to
532 water and ammonia fumigated feed based on vegetable protein *ad libitum*. The *Eimeria tenella*
533 Houghton (H) reference strain was used (63). Parasites were passaged by oral inoculation of
534 specified pathogen-free Lohmann Valo chickens, purified and prepared for use as described
535 elsewhere (50). At 21 days post-hatch, chicks were weighed and infected by oral inoculation
536 with 7000 sporulated *E. tenella* oocysts or mock-infected using sterile water. Group sizes
537 (minimum eight to ten per group) were determined following dose titration in IL10KO and
538 IL10EnKO HET chickens using power calculations with alpha set at 0.05 and power at 80%.
539 At the desired timepoint, birds were culled and whole blood was collected for serum. Caeca
540 were collected, scored for severity of infection (64) and preserved using RNAlater (Invitrogen).
541 Total genomic DNA (gDNA) was extracted from thawed complete caeca stored in RNAlater
542 from all studies. Caeca were homogenised in Buffer ATL using a TissueRuptor homogenizer
543 (Qiagen, Hilden, Germany) and then digested overnight at 56 °C in Buffer ATL and proteinase
544 K, prior to extraction using the Qiagen DNeasy Blood and Tissue DNA Kit according to
545 manufacturer's instructions.

546 Quantitative PCR for assessment of *E. tenella* genome copy number was performed as
547 previously described (65). Briefly, gDNA extracted from caecal tissue was used as template
548 for qPCR targeting *E. tenella* (RAPD-SCAR marker Tn-E03-116, primers F: 5'-
549 TCGTCTTTGGCTGGCTATTC-3', R: 5'-CAGAGAGTCGCCGTCACAGT-3'), normalised
550 against the number of chicken tata-binding protein (TBP) genomic copies detected (F: 5'-
551 TAGCCCGATGATGCCGTAT-3', R: 5'-GTTCCCTGTGTCGCTTGC-3'). Quantitative PCR
552 was performed in 20 µL reactions in triplicate containing 10 µL 2 × SsoFast EvaGreen

553 Supermix (Bio-Rad, Hercules, CA, USA), 1 µL of primers (F: 3 µM, R: 3 µM), 8 µL of molecular
554 biological grade water (Invitrogen) and 1 µL of gDNA, or water as negative control. Hard-
555 shelled 96-well reaction plates (Bio-Rad) were sealed with adhesive film (Bio-Rad) and loaded
556 into a Bio-Rad CFX qPCR cycler. Reactions were heated to 95°C for 2 min, prior to 40 cycles
557 consisting of 95°C for 15 s then 60°C for 30 s with a fluorescence reading taken after each
558 cycle. Melting curve analysis was performed for 15 s at 95°C, before cooling to 65°C for 60 s,
559 then heating to 95°C in 0.5°C increments for 0.5 s. Absolute quantification was performed
560 against a standard curve generated using serially diluted plasmid DNA containing the
561 amplicon of interest (EtenSCAR or ChickenTBP), to generate a standard curve ranging from
562 10^6 to 10^1 genome copies per mL. Parasite genome copy number was normalised by division
563 with host (chicken) genome copy number.

564 **Statistical analyses**

565 Minitab Statistical Software was used to analyse IL10 protein levels and nitric oxide production
566 in BMDMs using two-tailed unpaired t tests, growth curves were analysed using two-tailed
567 unpaired t tests or one-way ANOVA with Bonferroni multiple comparison tests, and
568 histopathological scores were analysed using Mann-Whitney U tests or Kruskal-Wallis tests.
569 Analysis of bacterial counts, histopathology, and heatmaps was performed with GraphPad
570 Prism software version 10.2.0. Data from multiplex RT-qPCR was analysed with GenEx6
571 software. The distribution of data was analysed by D'Agostino-Pearson and Shapiro-Wilk
572 normality tests. *Eimeria* replication and chicken body weight gain during parasite infection
573 were analysed using one-way ANOVA with Tukey's multiple comparison tests, and differences
574 in lesion scores were tested by Kruskal-Wallis with Dunn's multiple comparison tests. Bacterial
575 counts and histopathology scores were analysed by Mann-Whitney U tests or Kruskal-Wallis
576 tests. Fold change in transcript abundance was analysed by t tests using normalised data.

577 **Acknowledgements**

578 We thank staff at the National Avian Research Facility of the Roslin Institute, at the Moredun
579 Research Institute, and at the Biological Services Unit of the Royal Veterinary College, for
580 care and maintenance of the chickens used in this study.

581 **Funding**

582 This research was enabled by responsive mode funding from the Biotechnology & Biological
583 Sciences Research Council (BBSRC; grant references BB/P021638/1 (to DPB & FT) and
584 BB/P022049/1 (to AP, DH, KB, KW, MJM & MPS). The work was also supported by Cobb
585 Vantress-LLC (MJM, DM and KW; grant reference 13393976), a Roslin Institute Early Career
586 Researcher Grant (DM; grant reference 13302777) and by BBSRC Institute Strategic
587 Programme grants (grant references BBS/E/D/20002174 and BBS/E/RL/230002B).

588 **Author Contributions**

589 Designed research: AP, DPB, DAH, DM, FT, KB, KW, MJM, MPS, RCT
590 Performed research: AAA, DPB, DM, GSA, JJO, KB, LG, LT, MV, RCT, ZW
591 Contributed new reagents/analytic tools: MJM
592 Analysed data: AAA, DB, DPB, DAH, DM, JDP, LG, LV, MJM, MPS, RCT, ZW
593 Wrote the paper: DPB, DAH, DM, FT, MJM, MPS, RCT
594 Secured funding: AP, DPB, DAH, DM, FT, KB, KW, MJM, MPS

595 **Competing Interests**

596 MJM is inventor on patent application WO 2020074915 for the iCaspase9 surrogate host
597 chicken; the University of Edinburgh is the applicant. The other authors declare no competing
598 interests.

Data Availability Statement

All study data are included in the article and/or SI Appendix. IL10KO and IL10EnKO edited PGCs (HET and HOM) are cryopreserved and available to researchers under MTA.

References

1. M. Saraiva, P. Vieira, A. O'Garra, Biology and therapeutic potential of interleukin-10. *J Exp Med* **217** (2020).
2. R. Kuhn, J. Lohler, D. Rennick, K. Rajewsky, W. Muller, Interleukin-10-deficient mice develop chronic enterocolitis. *Cell* **75**, 263-274 (1993).
3. R. K. Sellon *et al.*, Resident enteric bacteria are necessary for development of spontaneous colitis and immune system activation in interleukin-10-deficient mice. *Infect Immun* **66**, 5224-5231 (1998).
4. K. N. Couper, D. G. Blount, E. M. Riley, IL-10: the master regulator of immunity to infection. *J Immunol* **180**, 5771-5777 (2008).
5. M. T. Rasquinha, M. Sur, N. Lasrado, J. Reddy, IL-10 as a Th2 cytokine: Differences between mice and humans. *J Immunol* **207**, 2205-2215 (2021).
6. L. Brockmann *et al.*, Molecular and functional heterogeneity of IL-10-producing CD4(+) T cells. *Nat Commun* **9**, 5457 (2018).
7. M. C. Pils *et al.*, Commensal gut flora reduces susceptibility to experimentally induced colitis via T-cell-derived interleukin-10. *Inflamm Bowel Dis* **17**, 2038-2046 (2011).
8. B. Bernshtein *et al.*, IL-23-producing IL-10Ralpha-deficient gut macrophages elicit an IL-22-driven proinflammatory epithelial cell response. *Sci Immunol* **4** (2019).
9. N. S. Redhu *et al.*, Macrophage dysfunction initiates colitis during weaning of infant mice lacking the interleukin-10 receptor. *Elife* **6** (2017).
10. E. Zigmond *et al.*, Macrophage-restricted interleukin-10 receptor deficiency, but not IL-10 deficiency, causes severe spontaneous colitis. *Immunity* **40**, 720-733 (2014).
11. M. C. Piazzon, G. Lutfalla, M. Forlenza, IL10, A tale of an evolutionarily conserved cytokine across vertebrates. *Crit Rev Immunol* **36**, 99-129 (2016).
12. L. Rothwell *et al.*, Cloning and characterization of chicken IL-10 and its role in the immune response to *Eimeria maxima*. *J Immunol* **173**, 2675-2682 (2004).
13. K. M. Russell *et al.*, Transcriptomic analysis of caecal tissue in inbred chicken lines that exhibit heritable differences in resistance to *Campylobacter jejuni*. *BMC Genomics* **22**, 411 (2021).
14. K. Boulton *et al.*, Phenotypic and genetic variation in the response of chickens to Eimeria tenella induced coccidiosis. *Genet Sel Evol* **50**, 63 (2018).
15. C. L. Swaggerty, I. Y. Pevzner, M. H. Kogut, Selection for pro-inflammatory mediators produces chickens more resistant to *Eimeria tenella*. *Poult Sci* **94**, 37-42 (2015).
16. F. Calenge *et al.*, QTL for resistance to *Salmonella* carrier state confirmed in both experimental and commercial chicken lines. *Anim Genet* **40**, 590-597 (2009).
17. S. B. Ghebremicael, J. R. Hasenstein, S. J. Lamont, Association of interleukin-10 cluster genes and *Salmonella* response in the chicken. *Poult Sci* **87**, 22-26 (2008).
18. M. Ballantyne *et al.*, Avian primordial germ cells are bipotent for male or female gametogenesis. *Front Cell Dev Biol* **9**, 726827 (2021).
19. J. Ioannidis *et al.*, Primary sex determination in birds depends on DMRT1 dosage, but gonadal sex does not determine adult secondary sex characteristics. *Proc Natl Acad Sci U S A* **118** (2021).
20. Z. Wu *et al.*, Development and function of chicken XCR1(+) conventional dendritic cells. *Front Immunol* **14**, 1273661 (2023).

21. A. Idoko-Akoh, M. J. McGrew, Generation of genome-edited chicken through targeting of primordial germ cells. *Methods Mol Biol* **2631**, 419-441 (2023).
22. D. A. Hume, E. Wollscheid-Lengeling, R. Rojo, C. Pridans, The evolution of the macrophage-specific enhancer (Fms intronic regulatory element) within the CSF1R locus of vertebrates. *Sci Rep* **7**, 17115 (2017).
23. M. Ballantyne *et al.*, Direct allele introgression into pure chicken breeds using Sire Dam Surrogate (SDS) mating. *Nat Commun* **12**, 659 (2021).
24. Z. Wu *et al.*, Analysis of the function of IL-10 in chickens using specific neutralising antibodies and a sensitive capture ELISA. *Dev Comp Immunol* **63**, 206-212 (2016).
25. S. Papoutsopoulou *et al.*, Impact of interleukin 10 deficiency on intestinal rpithelium responses to inflammatory signals. *Front Immunol* **12**, 690817 (2021).
26. G. Buchler *et al.*, Strain-specific colitis susceptibility in IL10-deficient mice depends on complex gut microbiota-host interactions. *Inflamm Bowel Dis* **18**, 943-954 (2012).
27. S. Devkota *et al.*, Dietary-fat-induced taurocholic acid promotes pathobiont expansion and colitis in Il10-/- mice. *Nature* **487**, 104-108 (2012).
28. D. C. Gunasekera *et al.*, The development of colitis in Il10(-/-) mice is dependent on IL-22. *Mucosal Immunol* **13**, 493-506 (2020).
29. L. M. Keubler, M. Buettner, C. Hager, A. Bleich, A multihit model: Colitis lessons from the interleukin-10-deficient mouse. *Inflamm Bowel Dis* **21**, 1967-1975 (2015).
30. R. J. Pandit *et al.*, Microbial diversity and community composition of caecal microbiota in commercial and indigenous Indian chickens determined using 16s rDNA amplicon sequencing. *Microbiome* **6**, 115 (2018).
31. S. Salavati Schmitz, J. P. Salgado, L. Glendinning, Microbiota of healthy dogs demonstrate a significant decrease in richness and changes in specific bacterial groups in response to supplementation with resistant starch, but not psyllium or methylcellulose, in a randomized cross-over trial. *Access Microbiol* **6** (2024).
32. A. H. Havelaar *et al.*, World Health Organization global estimates and regional comparisons of the burden of foodborne disease in 2010. *PLoS Med* **12**, e1001923 (2015).
33. S. Humphrey *et al.*, *Campylobacter jejuni* is not merely a commensal in commercial broiler chickens and affects bird welfare. *mBio* **5**, e01364-01314 (2014).
34. L. S. Mansfield *et al.*, C57BL/6 and congenic interleukin-10-deficient mice can serve as models of *Campylobacter jejuni* colonization and enteritis. *Infect Immun* **75**, 1099-1115 (2007).
35. B. M. Schultz *et al.*, Persistent *Salmonella enterica* serovar Typhimurium infection increases the susceptibility of mice to develop intestinal inflammation. *Front Immunol* **9**, 1166 (2018).
36. P. Vohra *et al.*, Evaluation of glycosylated FlpA and SodB as subunit vaccines against *Campylobacter jejuni* colonisation in chickens. *Vaccines (Basel)* **8** (2020).
37. D. Borowska *et al.*, Highly multiplexed quantitative PCR-based platform for evaluation of chicken immune responses. *PLoS One* **14**, e0225658 (2019).
38. R. R. Chaudhuri *et al.*, Comprehensive assignment of roles for *Salmonella* Typhimurium genes in intestinal colonization of food-producing animals. *PLoS Genet* **9**, e1003456 (2013).
39. D. P. Blake *et al.*, Genetic and biological characterisation of three cryptic *Eimeria* operational taxonomic units that infect chickens (*Gallus gallus domesticus*). *Int J Parasitol* **51**, 621-634 (2021).
40. A. Bremner *et al.*, Kinetics of the cellular and transcriptomic response to *Eimeria maxima* in relatively resistant and susceptible chicken lines. *Front Immunol* **12**, 653085 (2021).
41. S. A. Redpath, N. M. Fonseca, G. Perona-Wright, Protection and pathology during parasite infection: IL-10 strikes the balance. *Parasite Immunol* **36**, 233-252 (2014).
42. T. von Heyl *et al.*, Loss of alphabeta but not gammadelta T cells in chickens causes a severe phenotype. *Eur J Immunol* **53**, e2350503 (2023).

43. K. Boulton *et al.*, Dissecting the genomic architecture of resistance to *Eimeria maxima* parasitism in the chicken. *Front Genet* **9**, 528 (2018).
44. L. Freem *et al.*, Analysis of the progeny of sibling matings reveals regulatory variation impacting the transcriptome of immune cells in commercial chickens. *Front Genet* **10**, 1032 (2019).
45. Y. S. Bajagai *et al.*, Layer chicken microbiota: a comprehensive analysis of spatial and temporal dynamics across all major gut sections. *J Anim Sci Biotechnol* **15**, 20 (2024).
46. S. E. Winter *et al.*, Gut inflammation provides a respiratory electron acceptor for Salmonella. *Nature* **467**, 426-429 (2010).
47. A. W. L. Rogers, R. M. Tsolis, A. J. Baumler, *Salmonella* versus the microbiome. *Microbiol Mol Biol Rev* **85** (2021).
48. D. P. Blake *et al.*, Re-calculating the cost of coccidiosis in chickens. *Vet Res* **51**, 115 (2020).
49. E. L. Clark *et al.*, Cryptic *Eimeria* genotypes are common across the southern but not northern hemisphere. *Int J Parasitol* **46**, 537-544 (2016).
50. P. L. Long, B. J. Millard, L. P. Joyner, C. C. Norton, A guide to laboratory techniques used in the study and diagnosis of avian coccidiosis. *Folia Vet Lat* **6**, 201-217 (1976).
51. M. S. A. Rasheed, U. P. Tiwari, J. C. Jespersen, L. L. Bauer, R. N. Dilger, Effects of methylsulfonylmethane and neutralizing anti-IL-10 antibody supplementation during a mild *Eimeria* challenge infection in broiler chickens. *Poult Sci* **99**, 6559-6568 (2020).
52. J. M. Sand, M. K. Arendt, A. Repasy, G. Deniz, M. E. Cook, Oral antibody to interleukin-10 reduces growth rate depression due to *Eimeria* spp. infection in broiler chickens. *Poult Sci* **95**, 439-446 (2016).
53. M. K. Arendt, L. J. Knoll, M. E. Cook, Oral antibody to interleukin-10 receptor 2, but not interleukin-10 receptor 1, as an effective *Eimeria* species immunotherapy in broiler chickens. *Poult Sci* **98**, 3471-3480 (2019).
54. P. A. Lessard *et al.*, Improved performance of *Eimeria*-infected chickens fed corn expressing a single-domain antibody against interleukin-10. *Nat Food* **1**, 119-126 (2020).
55. A. Balic *et al.*, Visualisation of chicken macrophages using transgenic reporter genes: insights into the development of the avian macrophage lineage. *Development* **141**, 3255-3265 (2014).
56. J. Whyte *et al.*, FGF, Insulin, and SMAD signaling cooperate for avian primordial germ cell self-renewal. *Stem Cell Reports* **5**, 1171-1182 (2015).
57. M. Clinton, A rapid protocol for sexing chick embryos (*Gallus g. domesticus*). *Anim Genet* **25**, 361-362 (1994).
58. K. Labun *et al.*, CHOPCHOP v3: expanding the CRISPR web toolbox beyond genome editing. *Nucleic Acids Res* **47**, W171-W174 (2019).
59. J. P. Concordet, M. Haeussler, CRISPOR: intuitive guide selection for CRISPR/Cas9 genome editing experiments and screens. *Nucleic Acids Res* **46**, W242-W245 (2018).
60. A. Idoko-Akoh, L. Taylor, H. M. Sang, M. J. McGrew, High fidelity CRISPR/Cas9 increases precise monoallelic and biallelic editing events in primordial germ cells. *Sci Rep* **8**, 15126 (2018).
61. F. A. Ran *et al.*, Genome engineering using the CRISPR-Cas9 system. *Nat Protoc* **8**, 2281-2308 (2013).
62. D. M. McCafferty *et al.*, Spontaneously developing chronic colitis in IL-10/iNOS double-deficient mice. *Am J Physiol Gastrointest Liver Physiol* **279**, G90-99 (2000).
63. E. Aunin *et al.*, The complete genome sequence of *Eimeria tenella* (Tyzzer 1929), a common gut parasite of chickens. *Wellcome Open Res* **6**, 225 (2021).
64. J. Johnson, W. M. Reid, Anticoccidial drugs: lesion scoring techniques in battery and floor-pen experiments with chickens. *Exp Parasitol* **28**, 30-36 (1970).
65. M. J. Nolan, F. M. Tomley, P. Kaiser, D. P. Blake, Quantitative real-time PCR (qPCR) for *Eimeria tenella* replication--Implications for experimental refinement and animal welfare. *Parasitol Int* **64**, 464-470 (2015).

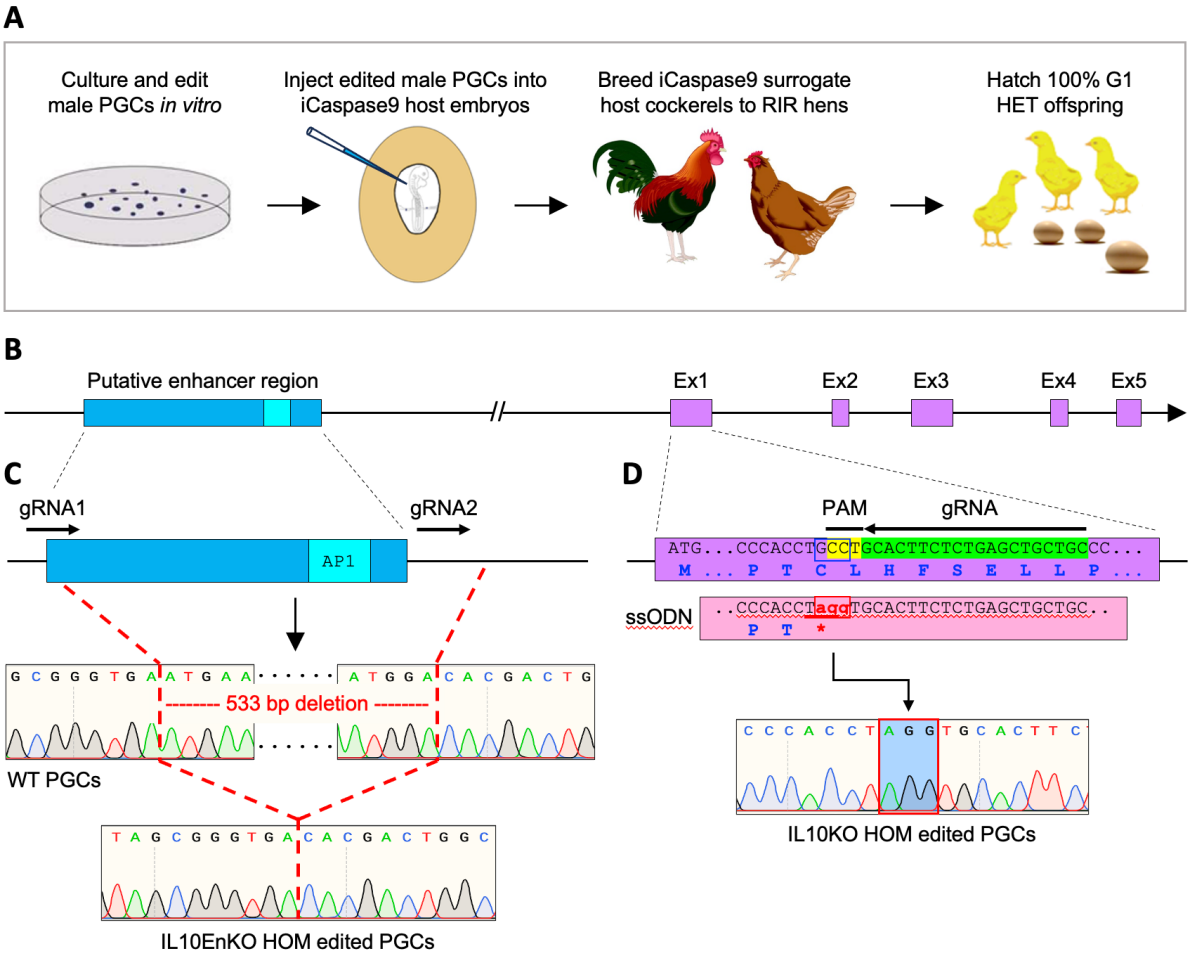

Figure 1: **IL10KO and IL10EnKO editing strategies. A**: Schematic of the pipeline used to create gene-edited chickens using embryonic PGCs and the iCaspase9 sterile surrogate host line. Male PGCs carrying the desired biallelic (HOM) edits were injected into iCaspase9 sterile surrogate host embryos to create IL10KO and IL10EnKO chickens. Upon sexual maturity, surrogate host cockerels were bred to RIR hens, resulting in 100% IL10KO HET or IL10EnKO HET offspring in the first generation (G1). **B**: Schematic of the *IL10* locus depicting the *IL10* putative enhancer region and the five *IL10* exons (Ex1 to Ex5). **C**: IL10EnKO HOM PGCs were created by deleting a 533-bp fragment encompassing the *IL10* putative enhancer region, using two gRNAs; DNA sequencing confirmed the biallelic deletion. **D**: IL10KO HOM PGCs were created using one gRNA and a 143-bp repair template (ssODN) to modify three nucleotides in *IL10* exon 1 (red, lowercase), thus introducing a premature in-frame stop codon in the *IL10* gene (underlined, *); DNA sequencing confirmed the biallelic edit.

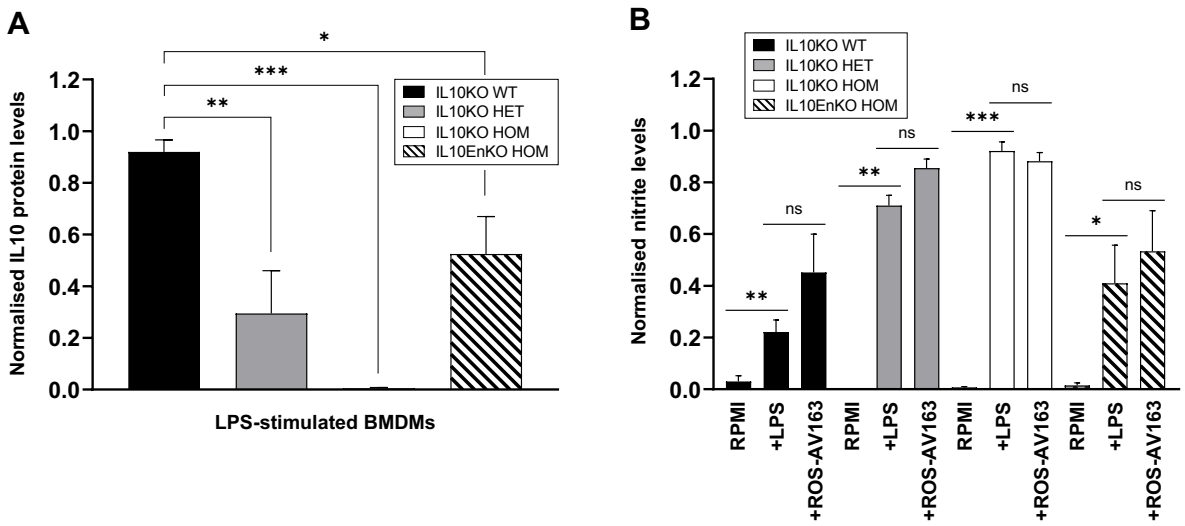

Figure 2: Confirmation of the IL10 mutation in bone marrow-derived macrophages. A: IL10 protein levels were measured by capture ELISA for LPS-stimulated BMDMs derived from Day 18 IL10KO WT (n=4), HET (n=2), HOM (n=4) and IL10EnKO HOM (n=4) embryos. Two independent experiments were performed and protein levels were normalised against the highest IL10KO WT value for each experiment and then combined. LPS treatment induced IL10 production in IL10KO WT BMDMs, but not in IL10KO HOM BMDMs; intermediate levels of IL10 were detected in IL10KO HET and IL10EnKO HOM BMDMs; IL10 expression in non-LPS induced samples was negligeable (<0.015; not shown). **B**: Nitric oxide production was assessed by measuring nitrite levels using Griess assay for LPS-stimulated BMDMs derived from Day 18 IL10KO WT (n=6), HET (n=2), HOM (n=7) and IL10EnKO HOM (n=6) embryos, in the absence or presence of neutralizing anti-IL10 antibody ROS-AV163. Three independent experiments were performed and nitrite levels were normalised against the highest IL10KO HOM nitrite value for each experiment before being combined. A significant increase in nitrite levels was observed in the absence of IL10 in IL10KO HOM BMDMs; nitrite levels were also increased in IL10KO HET and IL10EnKO HOM BMDMs. Addition of neutralizing anti-IL10 antibody did not significantly affect nitrite levels. Note that each BMDM sample was derived from three pooled embryos of the same genotype. Data displayed as mean with SE. Statistical significance calculated using two-tailed unpaired t tests; *$P < 0.05$, **$P < 0.01$, ***$P < 0.001$, ns: not significant.

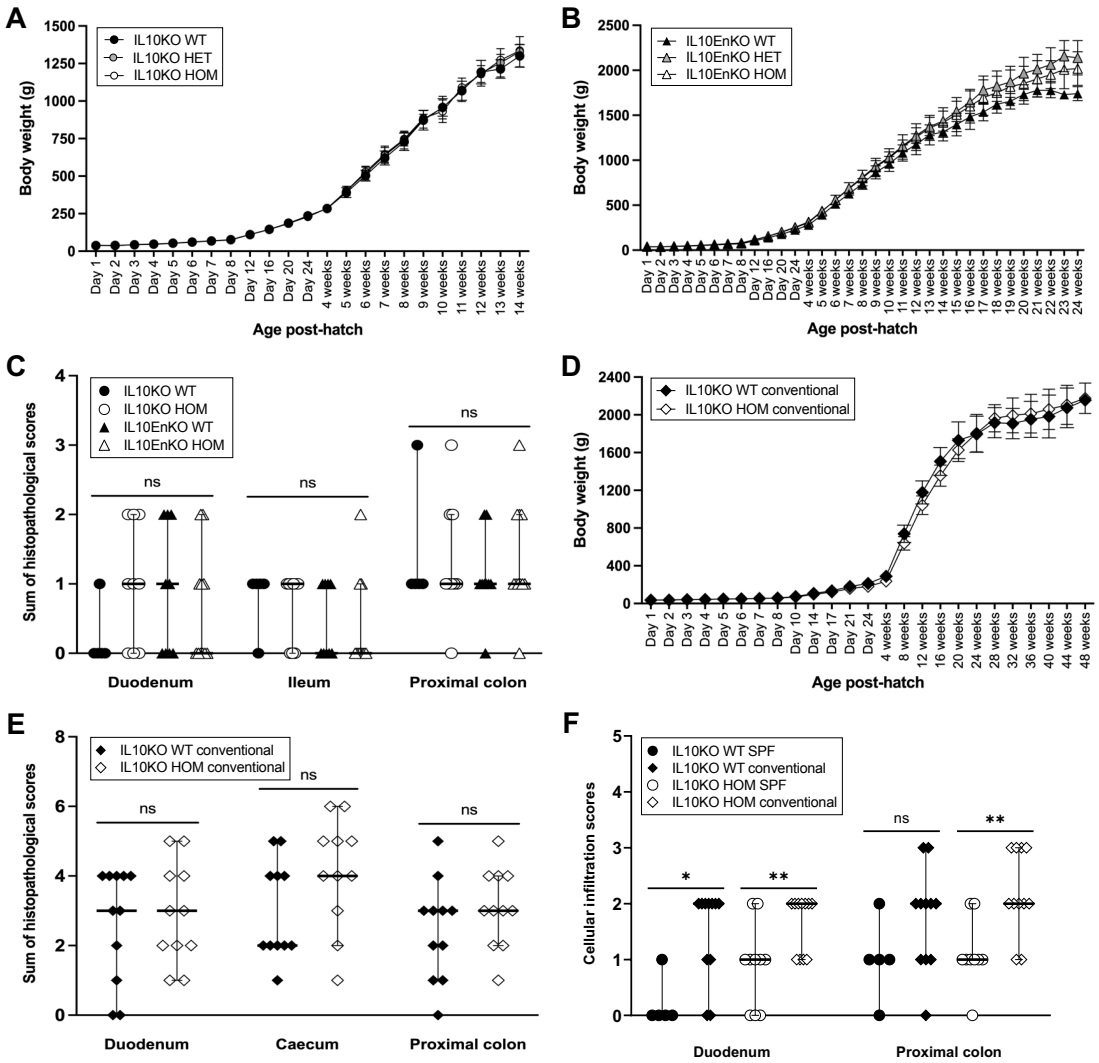

Figure 3: Growth curves and histopathological analyses of the gastrointestinal tract of IL10-deficient chickens in SPF and conventional facilities. A: Growth curves for IL10KO WT (n=3 to 8), HET (n=11 to 16) and HOM (n=2 to 4) hens raised in the NARF SPF facility, from hatch to 14 weeks. No significant weight differences were observed between genotypes at any timepoint ($P > 0.05$). **B**: Growth curves for IL10EnKO WT (n=2 to 4), HET (n=7 to 11) and HOM (n=5 to 11) hens raised in the NARF SPF facility, from hatch to 24 weeks. IL10EnKO HET and HOM hens were overall heavier than WT controls but this was statistically significant only between day 8 and day 24 ($P < 0.05$). **C**: Sums of histopathological scores for IL10KO WT (n=5) and HOM (n=9), and for IL10EnKO WT (n=9) and HOM (n=11) birds raised in the NARF SPF facility; tissue samples were collected at regular intervals from 16 to 40 weeks post-hatch. No significant differences were observed between genotypes for the tissues analysed. **D**: Growth curves for IL10KO WT (n=2 to 10) and HOM (n=5 to 15) hens raised in the NARF conventional facility, from hatch to 48 weeks. IL10KO HOM hens were significantly smaller than WT controls from 3 to 19 weeks post-hatch ($P < 0.05$), but this difference resolved with age. **E**: Sums of histopathological scores for IL10KO WT and HOM birds (n=11 in each group) raised in the NARF conventional facility; tissue samples were collected at regular intervals from 10 to 50 weeks post-hatch. No significant differences were observed between genotypes for the tissues analysed. **F**: Cellular infiltration scores for IL10KO WT and HOM birds raised in the NARF SPF and conventional facilities (same bird numbers as in C and E). Cellular infiltration scores were overall significantly higher for IL10KO WT and HOM birds raised in the conventional facility. Maximum possible sums of scores for data in C and E = 11; score range for data in F = 0 to 3. Data displayed as mean with SD (A, B and D) or as median with 95% confidence interval (C, E and F). Statistical significance calculated using one-way ANOVA with Bonferroni multiple comparison tests (A-B), Kruskal-Wallis test (C), two-tailed unpaired t tests (D), or Mann-Whitney U tests (E, F); *$P < 0.05$, **$P < 0.01$, ns: not significant.

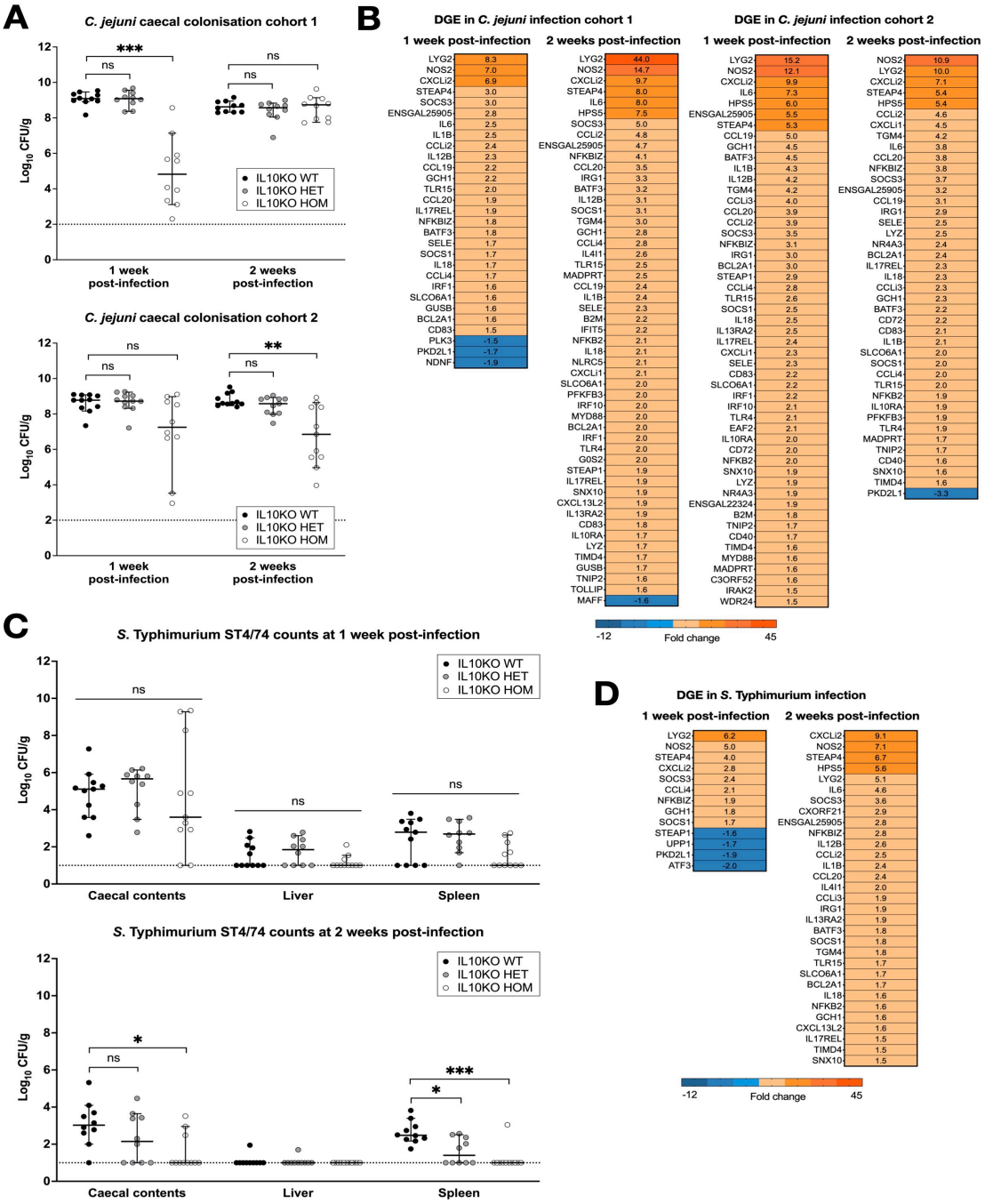

Figure 4: Net replication of *C. jejuni* and *S.* Typhimurium in the caeca of IL10KO WT, HET and HOM chickens and immune responses to infection. A: Caecal burden of *C. jejuni* strain M1 in IL1KO WT, HET and HOM chickens at 1- and 2-weeks post-inoculation in two separate trials. **B**: Heat map of differentially transcribed genes measured by multiplex qRT-PCR in the caeca of IL10KO HOM chickens in relation to IL10KO WT birds at 1- and 2-weeks post-inoculation in two separate trials. An increase in the expression of pro-inflammatory genes was consistently observed in both studies. **C**: Burden of S. Typhimurium strain ST4/74 in the caeca, liver and spleen of IL10KO WT, HET and HOM chickens at 1- and 2-weeks post-inoculation (single trial). **D**: Heat map of differentially transcribed genes in the caeca of IL10KO WT and HOM chickens 1- and 2-weeks post-inoculation with ST4/74. All group sizes: n=10 or 11. Bacterial colonisation shown as median with 95% confidence interval; dotted line shows limit of detection for each study (A, C). Statistical significance calculated using one-way ANOVA with Kruskal-Wallis test followed by Dunn's multiple comparison tests; *$P < 0.05$, **$P < 0.01$, ***$P < 0.001$, ns: not significant.

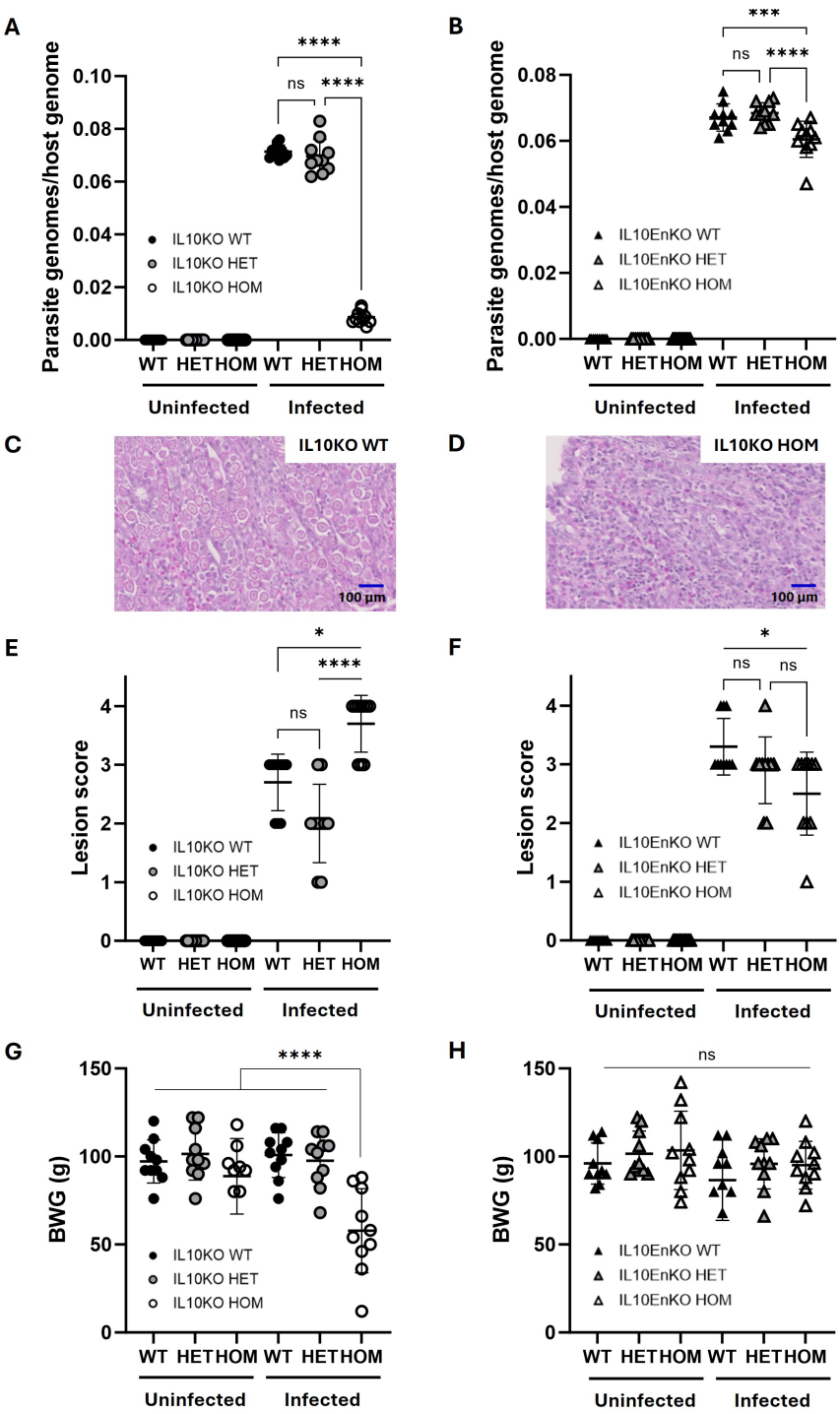

Figure 5: *Eimeria tenella* replication and impact on host pathology and performance in WT, HET and HOM G2 populations of IL10KO and IL10EnKO chickens. A-B: Parasite replication calculated as parasite genomes per host genome detected by quantitative PCR in genomic DNA extracted from caecal tissue six days post-infection (dpi). **C-D**: Haematoxylin and eosin stained caecal tissues collected from IL10KO WT and HOM chickens six days post *Eimeria tenella* infection. Numerous gametocytes are visible in the IL10KO WT line (C); gametocytes are largely absent in the IL10KO HOM line (D). **E-F**: Parasite-associated pathology measured as caecal lesion scores six dpi. **G-H**: Bodyweight gain (BWG) over six days from time of challenge to sampling. All group sizes: n=10. Statistical significance calculated using one-way ANOVA with Tukey's multiple comparison tests (A-B, G-H) or Kruskal-Wallis with Dunn's multiple comparison tests (E-F); *$P < 0.05$, ***$P < 0.001$, ****$P < 0.0001$, ns: not significant.

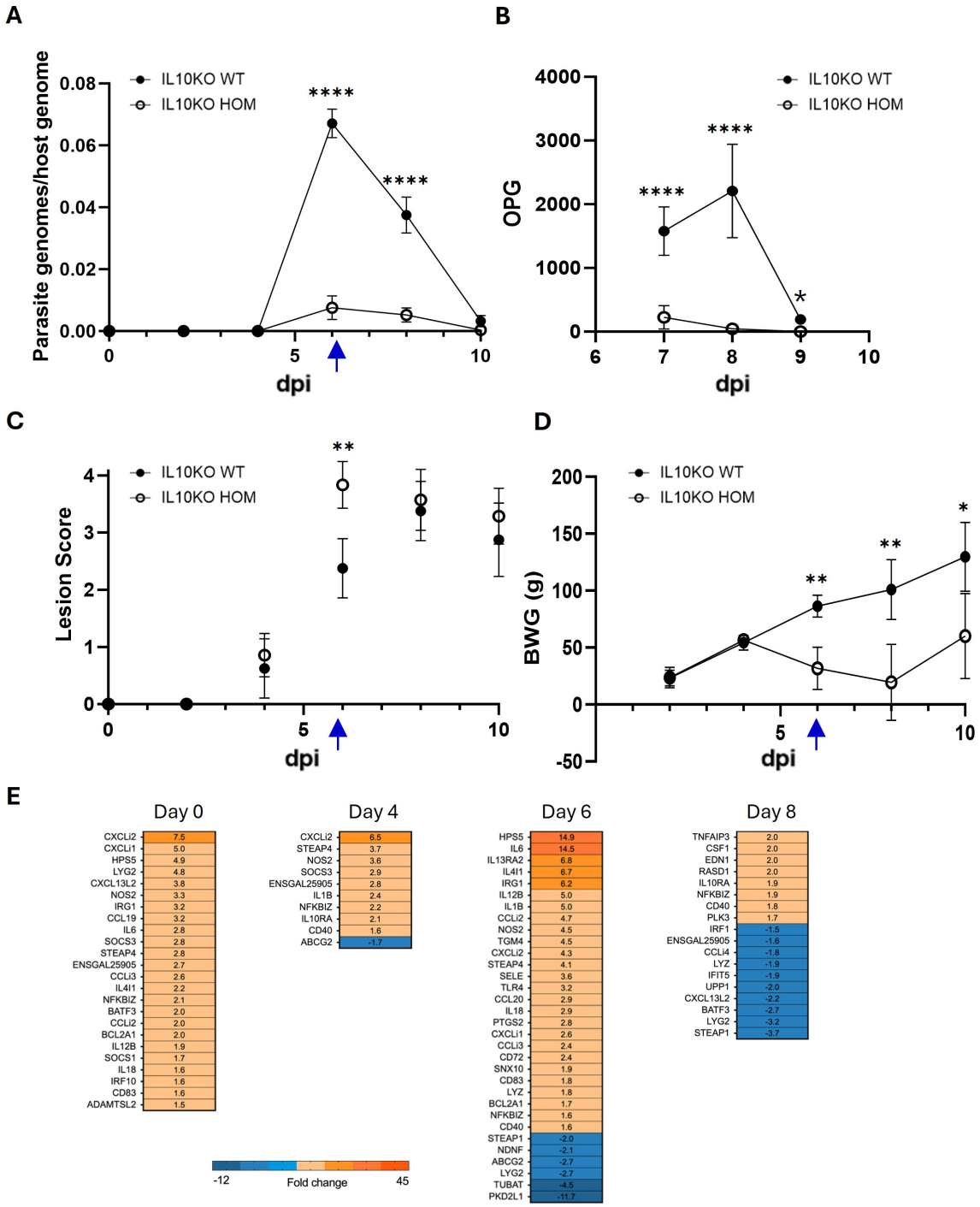

Figure 6: *Eimeria tenella* infection time course in IL10KO WT and HOM chickens. A: Parasite replication calculated as parasite genomes per host genome detected by quantitative PCR in genomic DNA extracted from caecal tissue. **B**: Oocysts per gram (OPG) litter. **C**: Parasite-associated pathology measured as caecal lesion scores. **D**: Bodyweight gain (BWG) over ten days from time of challenge to final sampling. **E:** Heat map of differentially transcribed genes in the IL10KO HOM caeca relative to IL10KO WT chickens 0-, 4-, 6- and 8-days post-infection (dpi). 48 chicks per group, eight culled from each group per timepoint. Statistical significance calculated using mixed-effects model (REML) with Tukey's multiple comparison tests (A, D), two-way ANOVA with Šídák's multiple comparison tests (B), or Mann-Whitney U tests (C); *$P < 0.05$, **$P < 0.01$, ***$P < 0.001$, ****$P < 0.0001$, ns: not significant. Blue arrows indicate the time of sampling in the comparative phenotyping study (Figure 5).